Induced Currents on a Moving and Vibrating Perfect Plane Under the Illumination of Electromagnetic Pulse: One-Dimensional Simulation using Characteristic-Based Algorithm

Mingtsu Ho
Department of Electronic Engineering, WuFeng Institute of Technology
117 Jian Kuo Road Section 2, Min Shong, Chia Yi, Taiwan
homt@mail.wfc.edu.tw

Abstract: This paper provides one-dimensional simulation results of the induced currents on constantly moving and vibrating perfect conductors under the normal illumination of plane Gaussian electromagnetic pulses. The characteristic-based algorithm is employed for the solutions of time-dependent Maxwell curl equations. In the numerical model, the size of the computational cell adjacent to the moving boundary, and its corresponding numerical time step become time-dependent since the boundary is not stationary. By comparing the computational results with the theoretical Doppler shift values, we show that the present method successfully predicts the induced currents on the perfect conductor surface. The computed electric and magnetic field intensities and induced currents are demonstrated as well.

***Introduction*:**

The effects on electromagnetic waves caused by uniformly traveling or oscillating targets are usually neglected if the velocity of movement or the resultant instantaneous speed of vibration is relatively small. The study of these topics becomes important wherever researchers have to deal with them. Several analytic studies can be found and the following remarks can be drawn: perfect conductors undergoing translational motion result in the well-known Doppler shift in the reflected fields; an oscillating target changes not only the phase but also the magnitude of the scattered fields [1–3].

A variety of computational techniques are developed for the solutions of the electromagnetic scattering problems for the past half century. The two most commonly approaches for solving electromagnetic problems are the method of moments (MoM) and the finite-difference time-domain (FDTD) technique. A recently proposed method applied to the solution of various electromagnetic problems is the characteristic-based algorithm that numerically approximates the time-dependent Maxwell curl equations. Whitfield and Janus applied this characteristic-based algorithm to the solutions of the Navier-Stokes equations for the fluid dynamic problems in the early 80s [4]. A decade later, Shang employed this method to solve the time-domain Maxwell's equations [5] through the application of explicit central-difference scheme. The implicit formulation was developed for the same purpose and its results were found to agree with data produced by FDTD [6]. Unlike MoM and FDTD, all field quantities are placed in the center of grid cell in the characteristic-based approach. It directly solves Maxwell's equations by balancing the net flux across all cell faces within each computational cell. The present numerical method is then considered a better approach over MoM and FDTD for problems involved with time varying cells, such as cases where object is moving or vibrating.

Governing Equations:

The governing equations for electromagnetic problems in source-free region are the time-dependent Maxwell curl equations:

$$\frac{\partial \mathrm{B}}{\partial \mathrm{t}} + \nabla \times \mathrm{E} = 0 \tag{1}$$

$$\frac{\partial \mathrm{D}}{\partial \mathrm{t}} - \nabla \times \mathrm{H} = 0 . \tag{2}$$

Since one-dimensional models are used, we can only consider a two-dimensional numerical formulation. To begin with, the characteristic-based algorithm requires the transformation of the governing equations from the

Cartesian coordinate system (t, x, y) into the body-fitted coordinate system (τ, ξ, η). We rewrite (1) and (2) as

$$\frac{\partial Q}{\partial \tau} + \frac{\partial F}{\partial \xi} + \frac{\partial G}{\partial \eta} = 0 \tag{3}$$

where

$$Q = J\, q \tag{4}$$

$$F = J\,(\xi_x f + \xi_y g) \tag{5}$$

$$G = J\,(\eta_x f + \eta_y g) \tag{6}$$

and

$$J = \left| \frac{\partial x}{\partial \xi}\frac{\partial y}{\partial \eta} - \frac{\partial x}{\partial \eta}\frac{\partial y}{\partial \xi} \right| . \tag{7}$$

The symbol J in above equations stands for the Jacobian of the inverse transformation, and the three variable vectors are respectively given by

$$q = [\, B_x\,,\, B_y\,,\, D_z\,]^T \tag{8}$$

$$f = [\, 0\,,\, -E_z\,,\, -H_y\,]^T \tag{9}$$

$$g = [\, E_z\,,\, 0\,,\, H_x\,]^T. \tag{10}$$

Shown as in (3) is called the Maxwell's equations in form of the Euler equation. The numerical procedure is formulated by applying the central difference operator

$$\delta_k(\varphi) = (\varphi)_{k+½} - (\varphi)_{k-½} \tag{11}$$

to (3). Then it becomes

$$\frac{Q^{n+1} - Q^n}{\Delta \tau} + \frac{\delta_i F}{\Delta \xi} + \frac{\delta_j G}{\Delta \eta} = 0\,. \tag{12}$$

In (11) the half-integer index represents the interface between two adjacent computational cells where flux is evaluated. The superscripts "n" and "n+1" on variable vector Q in (12) are two consecutive time levels. The numerical method approximates Maxwell's curl equation in curvilinear coordinate system by solving for the flux change for each grid cell within each numerical time step. The flux vector splitting technique and the Newton iterative method are also applied followed by the lower-upper approximate factorization scheme for the solution of the system of linear equations.

Boundary Conditions:

The boundary conditions (BC's) used in the present method are derived from the concepts of characteristic variable (CV) boundary conditions and the relativistic boundary conditions. According to the definition, every CV associates with one particular eigenvalue and is defined as the product of the instantaneous variable vector and the eigenvector corresponding to that particular eigenvalues [4]. Since every eigenvalue indicates the direction and velocity of the information propagating across the cell face, the use of CV for the evaluation of boundary variables should increase the accuracy of scheme. In order to incorporate the relativistic effects on the perfectly conducting surface, we combine the characteristic variable boundary conditions and the relativistic relation to evaluate the boundary values of variables. The relativistic boundary conditions are given by

$$\hat{n} \times \vec{E}^b = (\hat{n} \cdot \vec{v})\, \vec{B}^b \tag{13}$$

where $\vec{v}$ and $\hat{n}$ are the velocity and unit vector normal of the perfectly conducting surface, respectively. The superscript "b" stands for the boundary values of the electric and magnetic field variables evaluated right on the perfectly conducting surface. By definition, the CV arriving on the boundary is given by

$$CV^b = \hat{n} \times \vec{B} + \eta_o\, \vec{D} \tag{14}$$

with η_o being the impedance of free space and $\vec{B}$ and $\vec{D}$ are variables of the cell next to the boundary. Note that, this CV^b is tangential to the perfectly conducting surface and contains information propagating from the adjacent cell as indicated by the corresponding eigenvalue.

***The Problem*:**

The incident electromagnetic pulse used in the simulation is specified as follows. It is a Gaussian-windowed plane electromagnetic pulse with a cutoff level of 100 dB from the peak value, initially propagates in the positive x-direction in source-free region, and normally illuminates upon a perfect plane that is either at rest or in motion. This Gaussian electromagnetic pulse with its electric intensity being normalized to unity has a width of

about 1.902 ns measured from the center to $e^{-0.5}$.

For a motionless boundary, the grid system is stationary where the cell number and cell dimension are constant and uniform as shown in Figure 1(a). In the present simulation, due to the motion of boundary, both cell number and cell size are changing as time advances. As shown in Figures 1(b) and 1(c), provided that the cell immediate next to the moving boundary is the cell N, portion of the N^{th} cell may be truncated by the boundary at certain instance of time; and a moment later an extra fractional cell, the $(N+1)^{th}$, may be introduced into the grid system. The number of cells eliminated from or added into the grid system may be multiple and subjects to the oscillation amplitude and the grid density. These variations must be taken into account by updating the effective cell area and the resultant numerical time step to maintain decent accuracy of scheme.

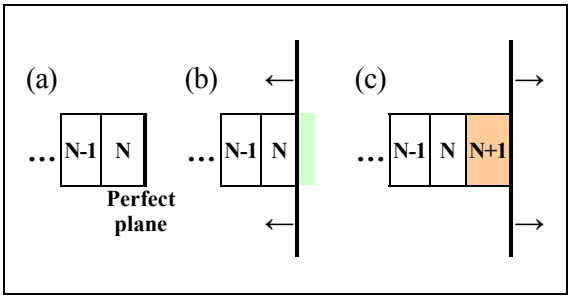

Figure 1. Computational cell indexing: (a) stationary grid system, (b) the N^{th} cell is truncated, (c) the $(N+1)^{th}$ cell is introduced.

In order to easily observe the effects of the moving object on the induced currents, we make the following arrangements. The perfectly conducting surfaces are set to constantly move at a velocity of 10 percent of the speed of light ($C = 3 \times 10^8$ m/s), and/or vibrate with a constant frequency and a constant amplitude so that the extreme instantaneous velocity equal to ± 0.1 C. The vibration frequency and amplitude are set to be 1 GHz (an impractical high value) and 4.775 mm to result in an extreme speed of 0.1 C near the equilibrium position. The resulting velocities of conductor are illustrated in Figure 2 where they are superposed if conductor moves and vibrates simultaneously. The two ratios of the translational velocity and oscillatory instantaneous velocity to the light speed are β_τ and β_v, respectively. Since the latter ranges from –0.1 C to +0.1 C, symbol $|\beta_v|$ is used for the magnitude. The value of β_τ and β_v is positive if conductor and the incident pulse move in the same direction and negative if they approach each other.

The numerical setups are as follows: the numerical electromagnetic pulse is plane and only has the components E_z and B_y. The excitation pulse is three meters in spatial span from the peak to the cutoff point; the number of grid cell for a six meters span is 800 points; the numerical time step is set so that the numerical electromagnetic pulse takes forty steps for one grid cell. Note that, for an oscillation amplitude as previously stated the moving boundary covers 1.273 cells peak-to-peak.

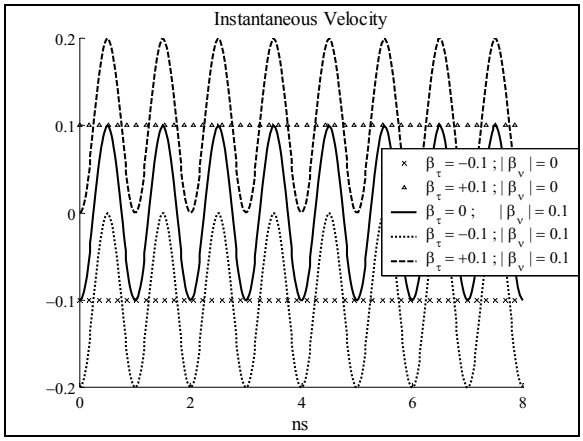

Figure 2. Instantaneous velocities of moving and/or vibrating conductors.

The induced currents are computed by taking the cross product of the unit vector normal and the magnetic field intensity where the latter is the resultant boundary values. Another field quantity sampled at the same location is the electric field intensity. If conductor is stationary the electric field is always zero in magnitude. Yet, the electric field is no longer vanished if conductor moves so that the relativistic effects cannot be dismissed. Under such circumstances, if the resultant velocity of conductor is $\vec{v}$, the boundary values of the field

components can be solved directly from equations (13) and (14) and are respectively given

$$\vec{B}^b = \frac{1}{\vec{v}-1} CV^b \qquad (15)$$

$$\vec{E}^b = \frac{\vec{v}}{\vec{v}-1} CV^b . \qquad (16)$$

To obtain above expressions, we take the convenience that both unit vector normal of the surface and velocity are along the x-axis. Note also that $\vec{v}$ used in (15) and (16) is the combined velocity of conductor and that the sign of this velocity is dependent upon the relativistic motion between the electromagnetic pulse and conductor as previously mentioned. The induced current flows in the positive z-direction can be computed as

$$\vec{J}_z = \hat{n} \times \vec{H}^b \qquad (17)$$

where $\vec{H}^b$ is the magnetic field intensity evaluated on the boundary.

***Results*:**

To illustrate the interaction between the electromagnetic pulse and the moving/vibrating perfect conductor, two time sequences of the electric field intensity are given in Figure 3. It is observed that on the perfectly conducting surface the electric fields are not always zero in strength due to the application of the relativistic boundary conditions. Plotted in Figures 4 and 5 are the boundary values of the electric and magnetic fields computed through (15) and (16). Note that all field quantities are normalized to unity henceforward and that the induced currents are similar to those of Figure 4 since it can be obtained by (17). If we take the difference between (15) and (16), we expect by the mathematical expression that the oscillatory behaviors of the fields would be cancelled out. The computational results are calculated and shown in Figure 6.

The Doppler effects on the induced current can be investigated on both magnitude and pulse width. The magnitude of the induced current is predictable by the relation $\frac{2}{1+(\beta_\tau+\beta_v)}$ and the resulted pulse width by $\sqrt{\frac{1-\beta_\tau}{1+\beta_\tau}}$ where the oscillatory behavior is ignored for easy estimation. Listed in Tables 1 and 2 are the calculated maximum shifts in magnitude along with the theoretical values. For instance, if the boundary moves and vibrates at the same time, when the maximum instantaneous velocity is –0.2 C, the corresponding magnitude is equal to 2.5; the pulse width is 1.2247 times that of the incident pulse, which is 1.7208. It is noted that the computational results are in good agreement with the analytical calculations.

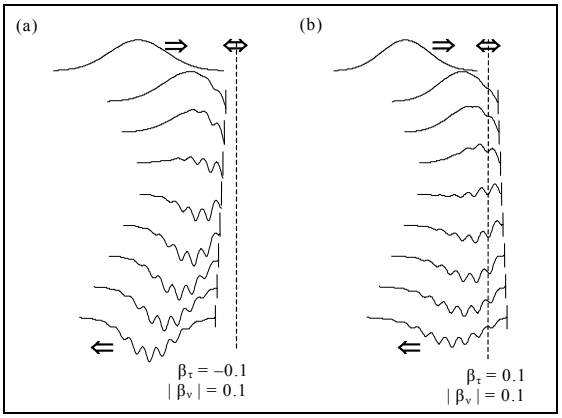

Figure 3. Interaction of electromagnetic pulse with moving perfect planes: (a) Vibrating and approaching, (b) Vibrating and receding (only electric fields are shown).

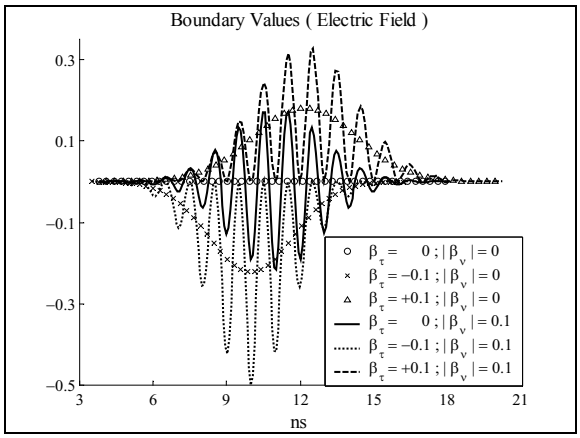

Figure 4. Calculated electric field using equation (3).

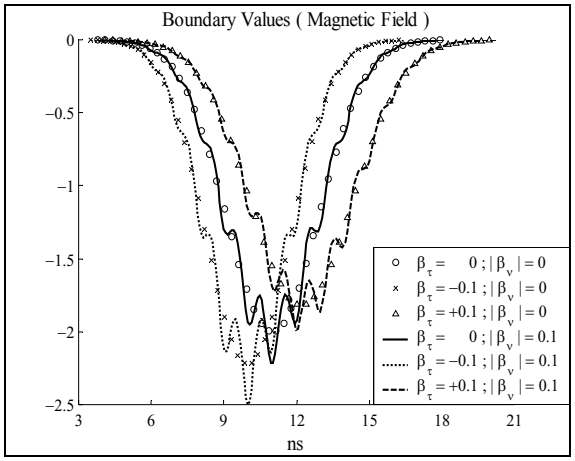

Figure 5. Calculated magnetic fields using equation (4).

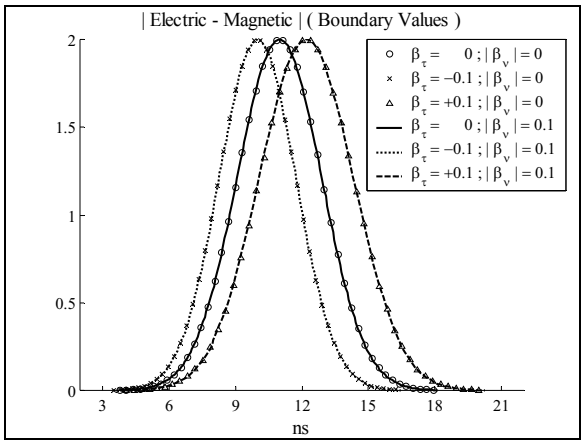

Figure 6. Magnitude of (E_z^b - H_y^b).

Table 1: Doppler shifts in pulse width.

Velocities		From center to $e^{-0.5}$	
β_τ	$\lvert \beta_v \rvert$	Calculated	Theoretical
0	0.0	1.9028	1.9024
− 0.1	0.0	1.7294	1.7208
+ 0.1	0.0	2.1153	2.1032

Table 2: Doppler shifts in the induced current.

Velocities		Maximum $\lvert J_z \rvert$	
β_τ	$\lvert \beta_v \rvert$	Calculated	Theoretical
0	0.0	1.9999	2.0000
− 0.1	0.0	2.2223	2.2222
+ 0.1	0.0	1.8176	1.8182
0	0.1	2.2220	2.2222
− 0.1	0.1	2.5001	2.5000
+ 0.1	0.1	1.9908	2.0000

***Conclusion*:**

This paper has shown that the characteristic-based algorithm successfully simulates the induced currents on the surface of moving and/or vibrating perfect conductors in one dimension. The computational results of the induced current magnitudes and pulse widths as consequences of the moving conductors are compared with the theoretical values. They are in good agreement. It is our future work to develop the existing code to problems with objects of finite dimension and problems involved with moving medium.

References

[1] R. E. Kleinman, R. B. Mack, "Scattering by linearly vibrating objects," IEEE Trans. Antennas Propagation, vol. AP-27, no. 3, pp. 344-352, May 1979.

[2] J. Cooper, "Scattering of electromagnetic fields by a moving boundary: the one-dimensional case," IEEE Trans. Antennas Propagation, vol. AP-28, no. 6, pp. 791-795, November 1980.

[3] F. Harfoush, A. Taflove, and G. Kriegsmann, "A numerical technique for analyzing electromagnetic wave scattering from moving surfaces in one and two dimensions," IEEE Trans. Antennas Propagation, vol. 37, pp. 55-63, January 1989.

[4] D. L. Whitfield and J. M. Janus, "Three-dimensional unsteady Euler equations solution using flux splitting," AIAA Paper, no. 84-1552, June 1984.

[5] J. S. Shang, "A characteristic-based algorithm for solving 3-d time-domain Maxwell equations," Electromagnetics, vol. 10, pp. 127, 1990.

[6] J. P. Donohoe, J. H. Beggs, and M. Ho, "Comparison of finite-difference time-domain results for scattered electromagnetic fields: Yee algorithm vs. a characteristic based algorithm," 27th IEEE Southeastern Symposium on System Theory, pp. 325-328, March 1995.

Mingtsu (Mark) Ho was born in Chia Yi City, Taiwan, R.O.C. in 1958. He received the B.S. degree in Physics in 1983 from the National Cheng Kung University, Tainan, Taiwan, R.O.C., the M.S. degrees in Physics and Electrical Engineering from the Mississippi State University, U.S.A., and the Ph.D. degree in Electrical Engineering from the Mississippi State University, U.S.A., in 1997.

He was a senior engineer in the R&D department, TECO Electric and Machinery Co., Ltd. from March 1998 till August 1999. Since then he has been an assistant professor in the Department of Electronic Engineering, Wufeng Institute of Technology, Chia Yi, Taiwan, R.O.C. His research interests include the use of the characteristic-based method for numerical simulations of the following problems: scattering of EM waves from moving/vibrating objects, EM interferences among strips, and the propagation of EM waves/pulses inside media having complex higher-order susceptibilities.